



## Original article

# Regulation of PKB/Akt-pathway in the chemopreventive effect of lactoferrin against diethylnitrosamine-induced hepatocarcinogenesis in rats



Rehab R. Hegazy<sup>a,\*</sup>, Dina F. Mansour<sup>a</sup>, Abeer A. Salama<sup>a</sup>, Rehab F. Abdel-Rahman<sup>a</sup>, Azza M. Hassan<sup>b</sup>

<sup>a</sup> Department of Pharmacology, Medical Division, National Research Centre, Giza, Egypt

<sup>b</sup> Department of Pathology, Faculty of Veterinary Medicine, Cairo University, Giza, Egypt

## ARTICLE INFO

## Article history:

Received 21 November 2018  
Received in revised form 15 April 2019  
Accepted 24 April 2019  
Available online 26 April 2019

## Keywords:

Hepatocellular carcinoma  
Diethylnitrosamine  
Lactoferrin  
Protein kinase B  
Vascular endothelial growth factor

## ABSTRACT

**Background:** Abnormal activation of protein kinase B (PKB) is associated with many cancers. This makes inhibition of PKB signaling pathway a promising strategy for cancer therapy. Lactoferrin (Lf) has been reported for its inhibition of tumor growth and metastasis, however, the mechanism is not completely understood. Its anti-hepatocarcinogenic activity has not taken the deserved recognition despite the additional advantages of Lf as an antiviral against hepatitis C virus, the main cause of hepatocellular carcinoma (HCC), and as a targeting ligand for delivering chemotherapeutics to hepatoma cells.

**Methods:** This study evaluated the anti-hepatocarcinogenic effect of Lf, and the role of PKB in this effect using diethylnitrosamine (DENA)-induced HCC rat model, and a primary cell culture prepared from the induced hepatic lesions (DENA–HCC cell culture).

**Results:** Up-regulation of activated PKB in the hepatocytes of rats with DENA-induced HCC was observed, as measured biochemically in the liver homogenate, and localized immunohistochemically. This was accompanied by increment of hepatocytes proliferation, and expression of vascular endothelial growth factor and endothelial nitric oxide synthase. Involvement of PKB in DENA-induced HCC was confirmed by the observed decrease in cell proliferation in DENA–HCC cell culture that was treated with PKB inhibitor. In Lf-treated rats, a dose-dependent chemopreventive effect was observed, with decreased expression and activation of PKB, amelioration of the other DENA-induced alterations, and stimulation of apoptosis. *In vitro*, Lf blocked PKB activator-induced cell proliferation.

**Conclusion:** These findings support the chemopreventive activity of Lf against HCC, and suggest regulation of PKB-pathway as a potential mechanism underlying this effect.

© 2019 Maj Institute of Pharmacology, Polish Academy of Sciences. Published by Elsevier B.V. All rights reserved.

## Introduction

Primary liver cancer is the fifth most common cancer worldwide, and the third cause of cancer-related death [1]. About 75–90% of liver cancers are hepatocellular carcinomas (HCC) [2]. One of the most leading causes of HCC is viral infection with hepatitis B and C viruses (HBV and HCV) [3]. About 70–80% of individuals infected with the virus become chronically infected, and, in its chronic form, hepatitis C can lead to liver fibrosis, HCC and eventually death from liver failure [4]. Other risk factors involved in the etiology of HCC include alcohol consumption,

obesity, environmental pollutants, and several dietary carcinogens, such as aflatoxins and nitrosamines [5,6]. Unfortunately, advanced HCC has limited approved treatment options and grave prognosis, therefore, chemoprevention has been considered as the best approach in lowering the high morbidity and mortality associated with this disease [7].

Lactoferrin (Lf) has attracted a lot of interest in the last few years due to its multi-pharmacological properties. It is a natural glycoprotein that found predominantly in milk and can also found in the other secretory fluids [8]. It has many pharmacological properties that are mediated through specific receptors [9]. Many recent studies have found promising anti-carcinogenic effects for Lf against a number of tumor cells [10–12]. However, the anti-tumor mechanism of Lf remains inconclusive. On the other hand, although it has been evaluated by some research groups [13,14],

\* Corresponding author.

E-mail address: [rehab\\_hegazy@hotmail.com](mailto:rehab_hegazy@hotmail.com) (R.R. Hegazy).

the antihepatocarcinogenic effect of Lf has not taken the much interest it deserves. In addition to its anti-cancer activity, Lf has been reported for its antiviral effect against HCV, the main cause of HCC, by preventing its binding to the host cells and preventing its replication [15]. More fascinatingly, many recent studies revealed that Lf could be used as a targeting agent to deliver chemotherapeutics to hepatoma cells, as it can bind to multiple receptors on hepatocytes [16]. Taken together, these important extra values of Lf necessitate a more extensive study of its antihepatocarcinogenic effect, due to the potential additional benefit that might be gained by using Lf in HCV patients susceptible to HCC, and in HCC patients as a drug delivery system.

Protein kinase B (PKB), also known as Akt, is a basic node in different signaling cascades that regulate the normal cellular physiology, and also involved in various disease conditions. It controls cell proliferation, growth, survival, glucose metabolism, and motility, as well as angiogenesis [17]. Increasing evidence suggests that abnormal activation of PKB is involved in human cancers and that inhibition of PKB signaling pathway might be a promising strategy for cancer treatment [18].

The current study aimed to evaluate the antihepatocarcinogenic effect of Lf against clinically relevant experimental rodent model of HCC, and to explore the role of PKB-pathway in this effect.

## Materials and methods

### Animals

Adult male Albino Wistar rats of 10–12 weeks, weighing 120–140 g, were obtained from the animal house colony of the National Research Centre (NRC, Egypt). The animals were maintained at a controlled temperature of  $24 \pm 1$  °C with a 12–12 h light–dark cycle (lights on at 0600–1800), and were allowed free access to water and standard chow *ad libitum*. They were treated according to the national and international ethics guidelines stated by the ethics committee of NRC, and all procedures and experiments were performed according to a protocol approved by it.

### Experimental design

Fifty-four rats were randomly allocated into five groups. The 1<sup>st</sup> group (n=6) received vehicles and served as the normal group (VHC). In the other four groups (n=12), HCC was induced according to Hussien et al. [19] with slight modifications. HCC was initiated using 1 monthly dose of diethylnitrosamine (DENA, Sigma Aldrich, USA) (200 mg/kg, *ip*) for 3 successive months. Following 2 weeks from the 1st DENA dose, phenobarbital (PhB, Sigma Aldrich, USA) was added daily to the drinking water of the rats (0.05%) till the end of the experiment to promote the hepatocarcinogenesis. The 2nd group served as an HCC model group; in the other 3 groups, rats received daily oral dose, by gavage, of Lf (Radiance Nutritional, New Zealand) dissolved in distilled water (100, 200, or 400 mg/kg/day) [20,21], respectively,

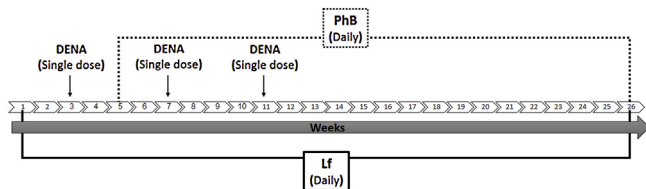


**Fig. 1.** Representative figure indicating induction and treatment regimen in rats. DENA, diethylnitrosamine (200 mg/kg, *ip*); PhB, phenobarbital (0.05% in the drinking water of the rats); Lf, lactoferrin (100, 200, or 400 mg/kg/day, *po*).

starting 14 days prior to DENA injection and till the end of the experiment (Fig. 1).

### Assessment of serum levels of liver function biomarkers

Twenty-four weeks following the 1st DENA injection, blood samples were withdrawn *via* tail vein of six rats per group under *ip* anesthesia with ketamine–xylazine (K, 100 mg/kg; X, 10 mg/kg) [22]. Serum was used for estimation of alanine aminotransferase (ALT) and aspartate aminotransferase (AST) activities, as well as bilirubin level, using specific kits (Biodiagnostic, Egypt).

### Morphometric analysis of hepatic nodulogenesis

Immediately after blood sampling, animals were sacrificed by cervical dislocation under K–X anesthesia, the livers were removed and grossly examined for presence of visible nodules, which appeared sharply demarcated and greyish-white. The sphere like nodules were measured in two perpendicular planes in order to get an average diameter for each nodule to the nearest millimeter. The visible nodules were classified into three categories relying on their diameter namely  $\geq 3$ ,  $<3$ – $<1$  and  $\leq 1$  mm, as described by Bishayee and Chatterjee [23]. The percentage of nodule incidence, the total number of nodules and the average number of nodules per nodule-bearing liver (nodule multiplicity) were calculated.

### Biochemical analysis of liver tissues

Following morphometric analysis, weighed parts from the livers and nodular lesions of six rats per group were homogenized (MPW-120 homogenizer, Med instruments, Poland). The homogenate was used for assessment of the contents of reduced glutathione (GSH) and lipid peroxides, measured as malondialdehyde (MDA), using Biodiagnostic kits (Egypt), glutathione-S-transferase (GST) and alpha-fetoprotein (AFP) using Bioneovan ELISA kits (China), lactate dehydrogenase (LDH) content using Salucea ELISA kits (Netherlands), as well as phosphorylate PKB and endothelial nitric oxide synthase (eNOS) levels using Systems ELISA kits (USA).

### Histopathological examination and histomorphometric analysis

Different tissue sections from liver and nodular lesions were fixed in 10% neutral buffered formalin, washed, dehydrated, and embedded in paraffin blocks. Sections of 5  $\mu$ m thickness were stained with haematoxylin and eosin (H&E) for histopathological examination. Five liver sections per group were examined. Ten random low microscopic fields (10X) per section were scanned for assessment of the histopathological lesions using binocular Olympus CX31 microscope. The pre-neoplastic and neoplastic lesions of liver were classified according to the method described previously [24]. For quantitative analysis of these pre-neoplastic and neoplastic hepatic lesions in H&E stained sections, the number and size of altered hepatic foci, hepatocellular adenoma and hepatocellular carcinoma were estimated in ten low microscopic fields (4X) according to published criteria [23,25]

### Immunohistochemical investigation

For immunostaining, the liver sections were deparaffinized and rehydrated in ethanol. The rehydrated sections were incubated in 0.3% hydrogen peroxide to inactivate endogenous peroxidase. The tissue sections were incubated with phosphorylated PKB (polyclonal antibody Ser473; Cell Signaling Technology Inc., USA), polyclonal anti-VEGF (Santa Cruz Biotechnology Inc., USA), polyclonal anti-caspase-3 (Abcam, Ltd., USA), and monoclonal

Anti-PCNA (Dako Corp, USA) as biotinylated primary antibodies. It was then incubated with biotin-conjugated secondary antibody (Vectastain ABC peroxidase kit, Vector Laboratories, USA). Diaminobenzidine (DAB) was used to demonstrate the immune reaction. Hepatocytes with brown cytoplasm were considered positive immune reactive cells for PKB, VEGF and caspase-3. Whereas, hepatocytes with brown nuclei were considered positive immune reactive cells for PCNA.

The immunohistochemical staining for PKB, VEGF proteins and Caspase-3 was assessed in ten random high microscopic power fields (40X) according to the method of Mae et al. [26] with some modifications. This assessment is

based on two main criteria including the color intensity and the percentage of positively immune stained cells. The color intensity was semi quantitatively graded from 0 to 3 in which grade 0 represent no staining, graded 1 represent weak staining, graded 2 represent moderate staining and graded 3 represent strong staining. Additionally, the percentage of positively stained cells was scored from 0 to 3, in which score 0 denotes 0%, score 1 denotes <30%, score 2 denotes 30%–70% and score 3 denotes >70%. The total immunoreactivity score (IRS) of each tissue section is the sum of the two criteria. IRS score < 4 is considered low expression and IRS score  $\geq 4$  is considered high [27].

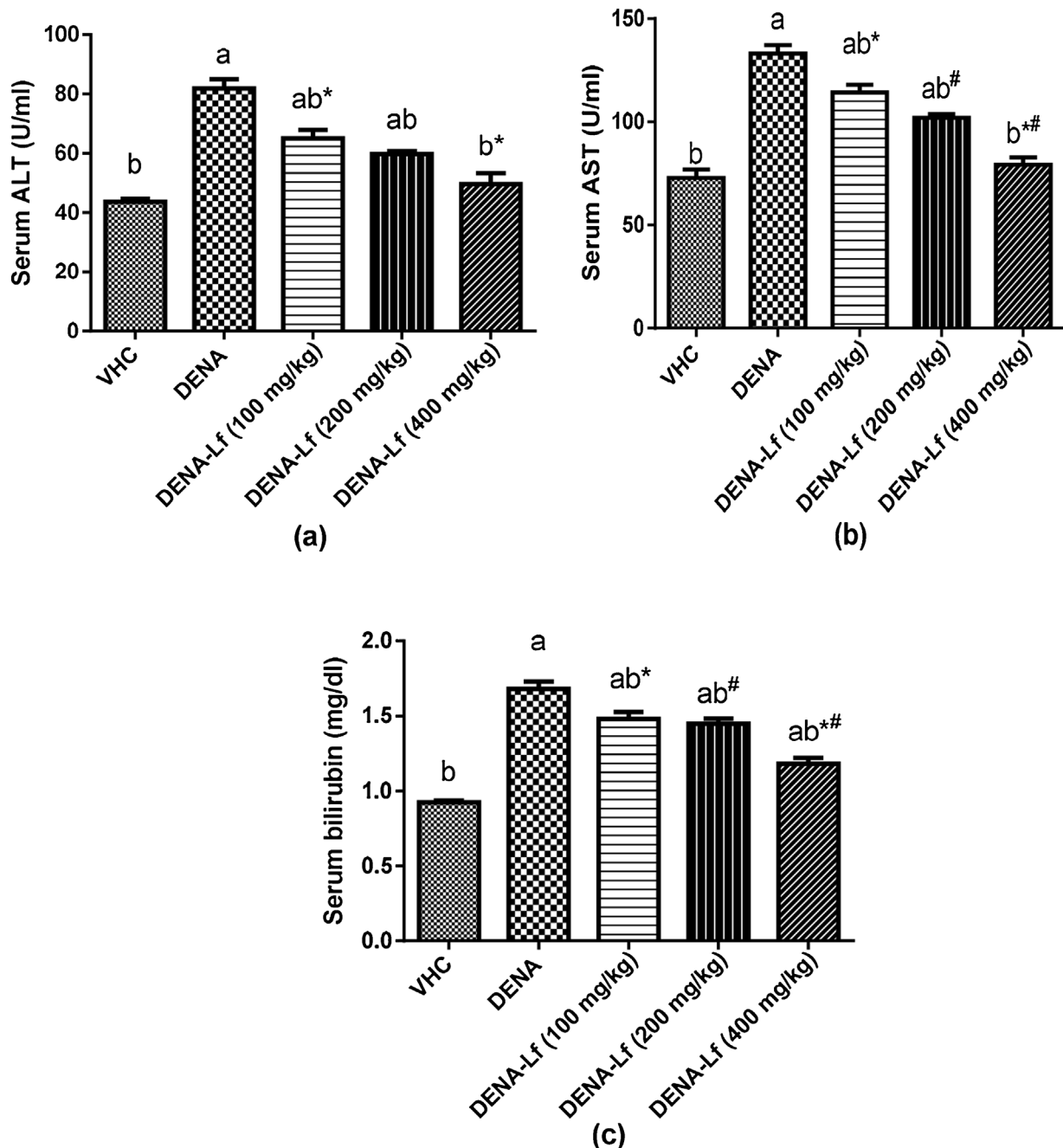


**Fig. 2.** Serum biomarkers of liver function. VHC, rats treated with vehicles; DENA, rats treated with diethylnitrosamine; DENA-Lf, rats treated with diethylnitrosamine and lactoferrin; ALT, alanine aminotransferase; AST, aspartate aminotransferase. Values represent the means  $\pm$  SE,  $n = 6$ . <sup>a</sup>Significantly different from VHC group at  $p < 0.05$ . <sup>b</sup>Significantly different from DENA group at  $p < 0.05$ . \*#DENA-Lf groups with the different symbol are significantly different from each other at  $p < 0.05$ .

On the other hand, the positively PCNA immune stained nuclei were counted in five random high microscopic field according to a method described before [21].

### The *in vitro* study

#### Preparation of primary cell culture

Tumor specimens from liver tissues of DENA-treated group that were not required for histopathological and immunohistochemical investigations, were used for further establishment of primary cell culture, named "DENA–HCC cells", according to the method described in a previous study with slight modifications [28]. Briefly, tumor sections were enzymatically digested by type IV collagenase (Sigma Aldrich, USA). The disaggregated cells were resuspended in Dulbecco's modified Eagle's medium (DMEM) supplemented with 10% fetal bovine serum (FBS) and penicillin-streptomycin (X100) (Lonza Group Ltd., Switzerland). Then, they were seeded onto 6-well culture plates coated with 0.1% gelatin to promote cell attachment and viability [29], incubated at 37 °C in 5% CO<sub>2</sub> and 95% humidity, and allowed to attach overnight prior to drug treatment.

#### Assessment of the role of PKB in the proliferation of DENA–HCC cells, and the effect of Lf on it

The following day DENA–HCC cells were treated (every 24 h for 5 days) with either 1 μM GSK690693 (a specific PKB inhibitor) [30] for 24 h/day, 10 μg/ml Lf [31] for 24 h/day, 100 nM insulin (a PKB activator) [32] for 30 min/day, or a combination of Lf and insulin at 37 °C in a humidified, 5% CO<sub>2</sub> atmosphere. In cells that were treated with insulin and Lf, they were pretreated every day with Lf for 23.5 h and subsequently cultured in DMEM containing 10% FBS and insulin for 30 min at 37 °C in a humidified, 5% CO<sub>2</sub> atmosphere. All drugs were dissolved in dimethyl sulfoxide (DMSO). DMSO was used as the negative control (CT). Insulin, GSK690693 and DMSO were purchased from Sigma-Aldrich (USA). At 1, 3, and 5 days after drug treatment, a cell count was made using a Bürker chamber and trypan blue dye (Sigma, USA) to differentiate live cells from dead.

To evaluate the role of PKB in DENA-induced HCC, the viability and proliferation of the negative control DENA–HCC cells were compared with those of the cells treated with specific PKB inhibitor, GSK690693.

On the other hand, to evaluate the potential direct inhibition of PKB by Lf, we compared the effects produced by the PKB activator (insulin) on the proliferation of DENA–HCC cells with that in Lf, and Lf/insulin-treated cell cultures.

#### Statistical analysis

All the values are presented as means ± standard error of the means (SE). Comparisons between different groups were carried out using one-way analysis of variance (ANOVA) followed by Tukey HSD test for multiple comparisons. Student *t*-test was used to compare the cell proliferation in negative control DENA–HCC and GSK690693-treated DENA–HCC cell culture. Graphpad Prism software, version 5 (Inc., USA) was used to carry out these statistical tests. The difference was considered significant when  $p < 0.05$ .

### Results

#### Serum levels of liver function biomarkers

DENA-induced HCC rat model markedly increased the normal serum activities of ALT and AST, as well as bilirubin level. Treatment of rats with Lf decreased this DENA-induced effect in

**Table 1**

Effect of Lf on the growth and development of nodules in the livers of DENA-treated rats.

Group	No. of rats with nodules / 6 rats	Nodule incidence	Total no. of nodules	Nodule multiplicity
VHC	–	–	–	–
DENA	6/6	100	107	17.3 <sup>a</sup> ±1.4
DENA-Lf (100 mg/kg)	4/6	66.6	45	11.25 <sup>b</sup> ±1.02
DENA-Lf (200 mg/kg)	3/6	50	27	9.00 <sup>c</sup> ±0.70
DENA-Lf (400 mg/kg)	2/6	33.3	11	6.50 <sup>d</sup> ±0.50

VHC, rats treated with vehicles; DENA, rats treated with diethylenitrosamine; DENA-Lf, rats treated with diethylenitrosamine and lactoferrin. Values represent the means ± SE. Groups with different superscript are significantly different at  $p < 0.05$ .

a dose-dependent manner, so as normal activities of ALT and AST were observed in Lf (400 mg/kg)-treated group, with a more significant improvement of bilirubin level compared to the other treated groups (Fig. 2).

#### Hepatic nodulogenesis

There was no definite apparent nodules in the liver of VHC group. Macroscopic nodules were clearly demonstrated on the surface of the livers of DENA-treated group. Table 1 illustrates the incidence of nodules, total number of nodules and nodule multiplicity (the average number of nodules per nodule-bearing liver) of DENA- and other treated groups. At 100 mg/kg, Lf treatment significantly reduced nodule incidence compared to DENA-treated group. Interestingly, pronounced decrease of nodule incidence was recorded in DENA-Lf (200 mg/kg) and DENA-Lf (400 mg/kg)-treated groups compared with DENA-treated one. The total number of nodules was markedly regressed in DENA-Lf (200 mg/kg) and DENA-Lf (400 mg/kg)-treated groups compared with DENA control. Additionally, diminished nodule multiplicity was recorded in Lf in a dose-dependent manner in comparison to DENA control group.

#### The size and distribution of visible nodules

Table 2 summarizes the size distribution of visible nodules in the liver of various treated groups. Lf treatment at 400 mg/kg significantly attenuated appearance of nodules ≥ 3 mm compared to DENA control group. Furthermore, increased number of nodules less than 1 mm was recorded in DENA-Lf (200 mg/kg) and DENA-Lf (400 mg/kg)-treated groups.

#### Hepatic oxidative stress markers

The normal hepatic oxidative index was altered in the rats with DENA-induced HCC model, as revealed by the elevated MDA content

**Table 2**

Effect of Lf on nodules size in the livers of DENA-treated rats.

Group	No. of rats	Nodules relative to size (% of total no.)		
VHC	–	≥3 mm	<3–<1 mm	≤1 mm
DENA	6	48 <sup>a</sup> ± 2	26 <sup>c</sup> ± 2	26 <sup>c</sup> ± 2
DENA-Lf (100 mg/kg)	4	38 <sup>b</sup> ± 4	32 <sup>b</sup> ± 3	30 <sup>b</sup> ± 3
DENA-Lf (200 mg/kg)	3	32 <sup>b</sup> ± 4	32 <sup>b</sup> ± 3	36 <sup>a</sup> ± 3
DENA-Lf (400 mg/kg)	2	30 <sup>c</sup> ± 3	35 <sup>a</sup> ± 2	35 <sup>a</sup> ± 4

VHC, rats treated with vehicles; DENA, rats treated with diethylenitrosamine; DENA-Lf, rats treated with diethylenitrosamine and lactoferrin. Values represent the means ± SE. Groups with different superscript are significantly different at  $p < 0.05$ .

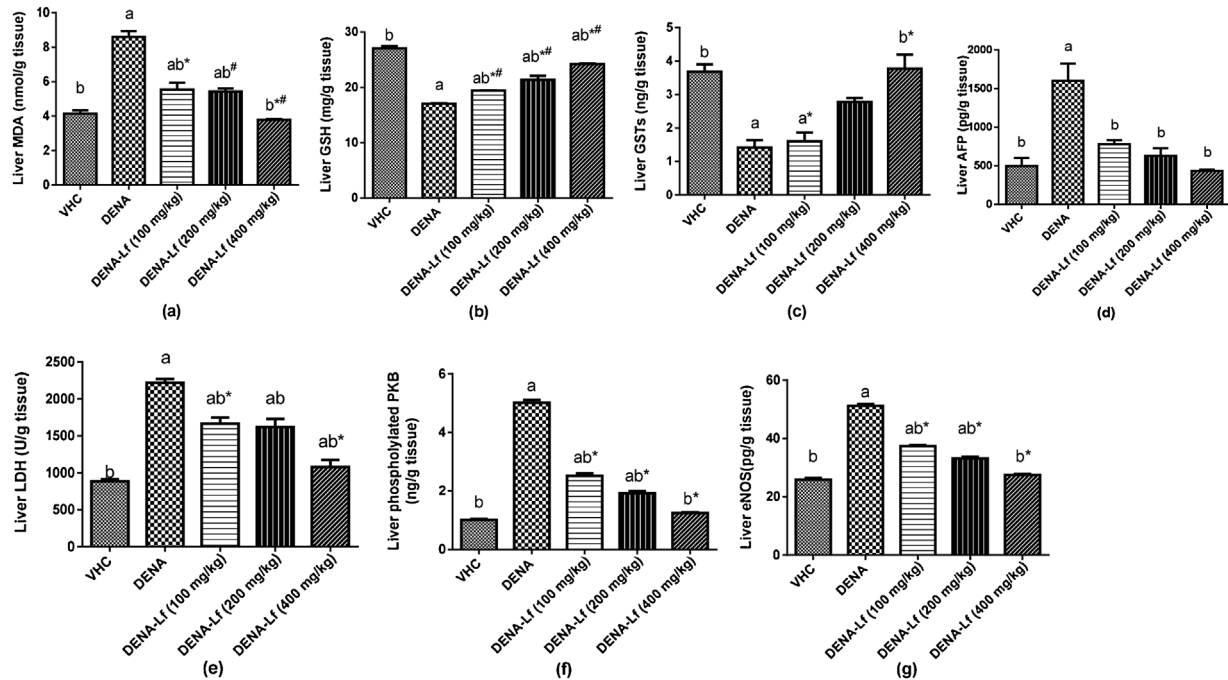


**Fig. 3.** The biochemical analysis of the liver contents of (a) MDA, (b) GSH, (c) GST, (d) AFP, (e) LDH, (f) PKB, and (g) eNOS. VHC, rats treated with vehicles; DENA, rats treated with diethylnitrosamine; DENA-Lf, rats treated with diethylnitrosamine and lactoferrin; MDA, malondialdehyde; GSH, glutathione; GST, glutathione-S-transferase; AFP, alpha-fetoprotein; LDH, lactate dehydrogenase; PKB, protein kinase B; eNOS, endothelial nitric oxide synthase. Values represent the means  $\pm$  SE,  $n = 6$ . <sup>a</sup>Significantly different from VHC group at  $p < 0.05$ . <sup>b</sup>Significantly different from DENA group at  $p < 0.05$ . <sup>\*</sup><sup>#</sup>DENA-Lf groups with the different symbol are significantly different from each other at  $p < 0.05$ .

and the decreased GSH and GST levels. Lf significantly retrieved the altered levels of MDA, GSH, and GST, with the most protective effect observed in the group treated with Lf (400 mg/kg) (Fig. 3a–c).

#### Hepatic tumor markers

DENA resulted in recognition of high levels of AFP and LDH in liver tissue homogenate of the rats. All doses of Lf normalized the level of AFP, while there was a dose-dependent protection against DENA-induced elevation of LDH (Fig. 3d and e).

#### The levels of phosphorylated PKB and eNOS in the liver

Significantly elevated levels of phosphorylated PKB and eNOS were demonstrated in rats with DENA-induced HCC. Treatment of the animals with Lf dose dependently suppress these effects, with conservation of the normal levels in rats treated with Lf (400 mg/kg) (Fig. 3f and g).

#### Hepatic architecture in rats

The detailed hepatocellular lesions demonstrated in the liver of DENA and Lf (100–200–400 mg/kg)-treated groups were summarized in Table 3. Liver of VHC treated rats showed normal hepatic architecture with preserved lobular pattern (Fig. 4a and b). Meanwhile, liver of DENA-treated group revealed distortion of the hepatic architecture with preneoplastic and neoplastic (hepatocellular adenoma) lesions as well as various multinodular carcinomatous lesions (Fig. 4c), in which the neoplastic cells arranged in solid sheet with cellular and nuclear pleomorphism in addition to presence of cytoplasmic inclusions including abundant globular eosinophilic inclusions and faint pink fibrinogen inclusion (Fig. 4d). The other commonly demonstrated hepatic lesions were neoplastic nodules and altered hepatic foci that were found all over the hepatic parenchyma. The neoplastic nodules (adenoma) were of large sized, disrupt, and compress the surrounding parenchyma. In addition, the plates of these nodules are discontinuous with those of the adjacent liver tissue. However, the altered foci are

**Table 3**  
The histopathological lesions demonstrated in the different groups of rats.

Groups	Altered foci		Hepatocellular adenoma		Hepatocellular carcinoma	
	Number /LPF	Mean area (mm <sup>2</sup> /cm <sup>2</sup> )	Number /LPF	Mean area (mm <sup>2</sup> /cm <sup>2</sup> )	Number /LPF	Mean area (mm <sup>2</sup> /cm <sup>2</sup> )
DENA	7.00 <sup>a</sup> +0.63	0.09 <sup>a</sup> +0.02	5.90 <sup>a</sup> +0.67	0.08 <sup>a</sup> +0.01	2.90 <sup>a</sup> +0.27	0.35 <sup>a</sup> +0.07
DENA-Lf (100 mg/kg)	5.30 <sup>b</sup> +0.83	0.03 <sup>b</sup> +0.01	4.30 <sup>b</sup> +0.36	0.06 <sup>b</sup> +0.01	0.80 <sup>b</sup> +0.24	0.12 <sup>b</sup> +0.04
DENA-Lf (200 mg/kg)	3.40 <sup>c</sup> +0.60	0.02 <sup>b</sup> +0.04	2.40 <sup>c</sup> +0.33	0.05 <sup>c</sup> +0.03	0.40 <sup>c</sup> +0.22	0.04 <sup>c</sup> +0.01
DENA-Lf (400 mg/kg)	0.40 <sup>d</sup> +0.34	0.03 <sup>c</sup> +0.01	0.10 <sup>d</sup> +0.10	0.01 <sup>c</sup> +0.02	0.10 <sup>d</sup> +0.10	0.02 <sup>c</sup> +0.01

VHC, rats treated with vehicles; DENA, rats treated with diethylnitrosamine; DENA-Lf, rats treated with diethylnitrosamine and lactoferrin. Values represent the means  $\pm$  SE. Groups with different superscript are significantly different at  $p < 0.05$ .

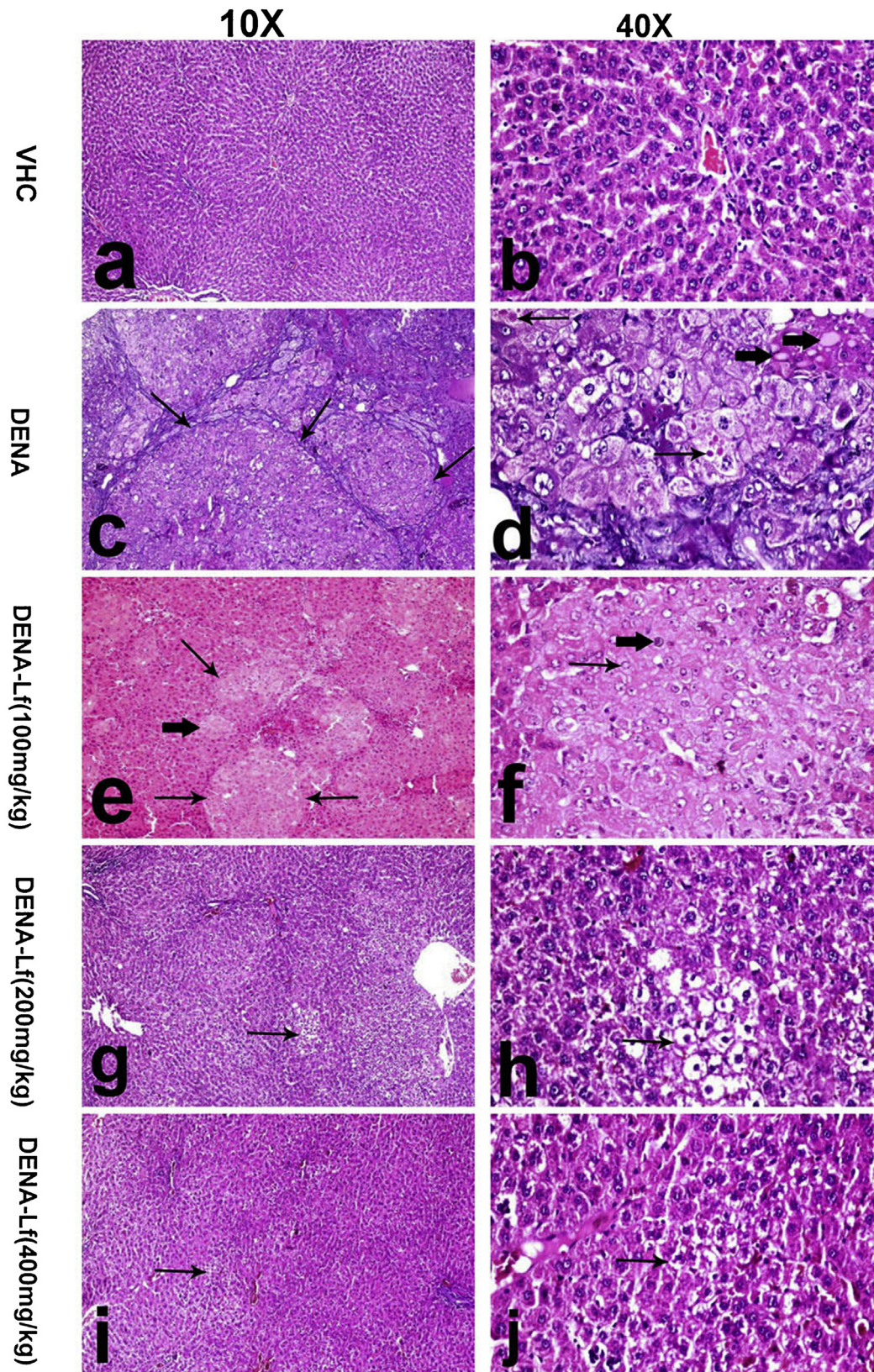


**Fig. 4.** Effect of Lf on the histopathological features of liver tissues of rats with DENA-induced HCC. VHC, rats treated with vehicles; DENA, rats treated with diethylenitrosamine; DENA-Lf, rats treated with diethylenitrosamine and lactoferrin. Photomicrograph of liver tissue of (a and b) VHC-treated rats showing normal hepatic architecture, (c and d) DENA-treated rats showing multi nodular hepatocellular carcinoma (arrows) (c) and large polygonal tumor cells with abundant intracytoplasmic eosinophilic globular inclusions (arrows), and fibrinogen inclusions (thick arrows, insert) (d), (e and f) DENA-Lf (100 mg/kg)-treated rats showing multiple large (arrows) and small altered hepatocellular foci (thick arrow) (e) characterized by multiple glycogenated nuclei (arrow) and prominent nucleoli (thick arrow) (f), (g and h) DENA-Lf (200 mg/kg)-treated rats showing small clear cell focus (arrows), and (i and j) DENA-Lf (400 mg/kg)-treated rats showing restoration of hepatic parenchyma (i) with vacuolation of hepatocellular cytoplasm (arrows) (j). (H&E; a, c, e, g and i X10; b, d, f, h and j X40).

**Table 4**

The results of immunohistochemical assays recorded in the liver of the different groups of rats.

Parameter	PKB (IRS)	VEGF (IRS)	Caspase-3 (IRS)	PCNA (count/ high microscopic field)
VHC	1.70 <sup>b</sup> ±0.21	1.60 <sup>b</sup> ±0.16	0.27 <sup>b</sup> ±0.27	0.60 <sup>b</sup> ±0.24
DENA	5.10 <sup>a</sup> ±0.27	3.40 <sup>a</sup> ±0.42	3.50 <sup>a</sup> ±0.40	89.40 <sup>a</sup> ±5.09
DENA-Lf (100 mg/kg)	3.90 <sup>ab*</sup> ±0.17	2.80 <sup>ab*</sup> ±0.38	3.55 <sup>ab*</sup> ±0.24	49.20 <sup>ab*</sup> ±5.81
DENA-Lf (200 mg/kg)	2.60 <sup>ab#</sup> ±0.22	2.30 <sup>ab#</sup> ±0.36	5.10 <sup>ab#</sup> ±0.27	17.40 <sup>ab#</sup> ±2.20
DENA-Lf (400 mg/kg)	1.40 <sup>b#</sup> ±0.42	1.80 <sup>b#</sup> ±0.24	5.30 <sup>ab#</sup> ±0.21	9.40 <sup>ab#</sup> ±1.29

VHC, rats treated with vehicles; DENA, rats treated with diethylenitrosamine; DENA-Lf, rats treated with diethylenitrosamine and lactoferrin; PKB, protein kinase B; VEGF, vascular endothelial growth factor; PCNA, proliferating cell nuclear antigen; IRS, the total immunoreactivity score. Values represent the means ± SE. \*, #, @ DENA-Lf groups with the different symbol are significantly different at  $p < 0.05$ .

<sup>a</sup> Significantly different from VHC group at  $p < 0.05$ .

<sup>b</sup> Significantly different from DENA group at  $p < 0.05$ .

small lesions of hepatocytes that don't disrupt the parenchymal architecture. Basophilic and clear foci were most abundant. The cells of these foci have round nuclei with prominent nucleoli. Glycogenated nuclei were also evident. LF Treatment revealed significant regression of preneoplastic and neoplastic lesions in a

dose-dependent manner. DENA-Lf (100 mg/kg)-treated group revealed significant decrease of number and size of neoplastic nodules and the lesions were mainly consisted of numerous AHF that appeared with increased size and weakly disarrange the hepatic parenchyma (Fig. 4e and f). On the other hand, the number

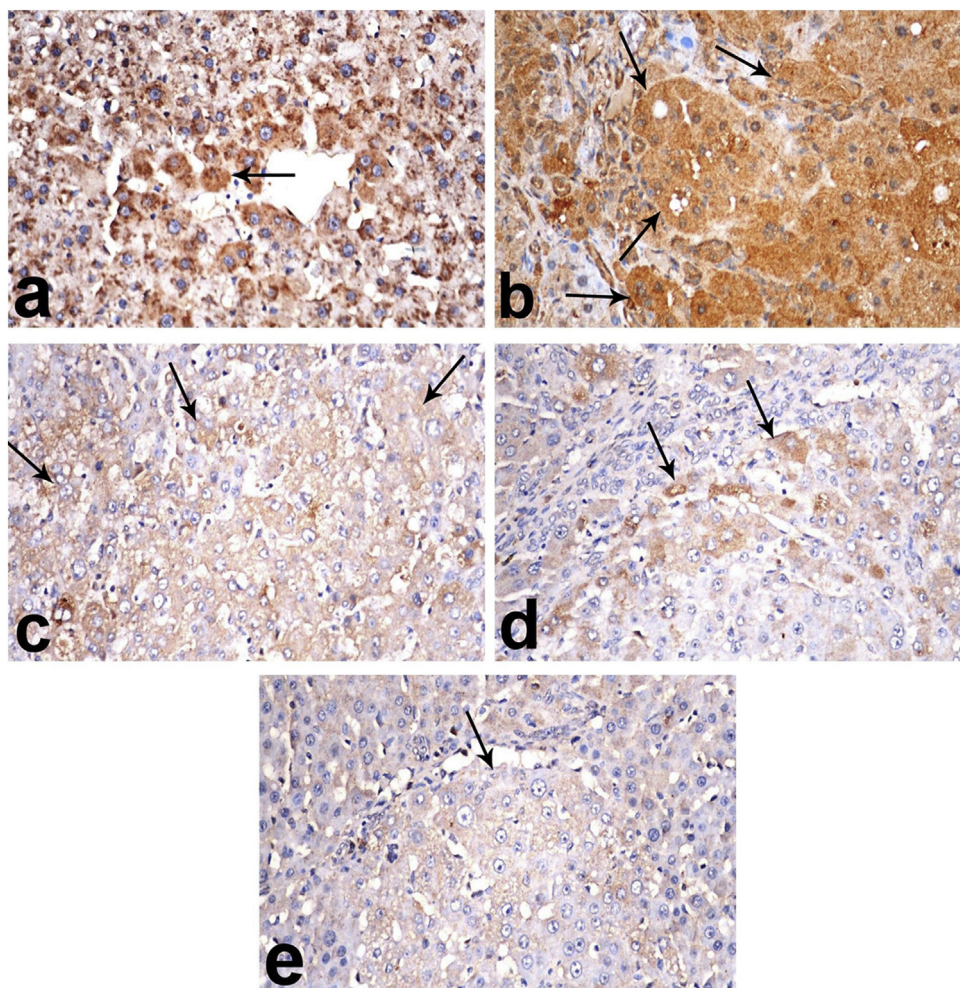


**Fig. 5.** PKB immunohistochemical staining of liver tissues. VHC, rats treated with vehicles; DENA, rats treated with diethylenitrosamine; DENA-Lf, rats treated with diethylenitrosamine and lactoferrin; PKB, protein kinase B. (a) VHC-treated rats showing cytoplasmic expression of PKB (arrow), (b) DENA-treated rats showing tumor nodule with strong cytoplasmic expression of PKB (arrow), (c) DENA-Lf (100 mg/kg)-treated rats showing moderate cytoplasmic expression (arrow), (d) DENA-Lf (200 mg/kg)-treated rats showing cytoplasmic expression in few immune stained cells (arrow), and (e) DENA-Lf (400 mg/kg)-treated rats showing weak expression (arrow) (PKB-immunohistochemical staining, X40).

and size of altered foci were diminished in DENA-Lf (200 mg/kg)-treated group and few small clear hepatocellular foci, that don't disrupt the hepatic architecture, were observed (Fig. 4g and h). Remarkable regression of preneoplastic lesions with pronounced delay of tumor development was demonstrated in DENA-Lf (400 mg/kg) treated group, in which marked restoration of hepatic parenchyma with few altered hepatocytes was demonstrated (Fig. 4i and j).

#### PKB immunohistochemical staining

Table 4 summarizes the results of immunohistochemical assay recorded in the liver of different groups.

#### PKB immunohistochemical staining

Positive AKT immune reactivity with cytoplasmic expression was demonstrated in the liver of VHC group (Fig. 5a). In contrast, the intensity and the percentage of positively immune stained cells were significantly increased in DENA-treated group (Fig. 5b), with mean IRS of  $5.10 \pm 0.27$ . Moderate staining was demonstrated in DENA-Lf (100 mg/kg)-treated group (Fig. 5c), with mean IRS of  $3.90 \pm 0.17$ . PKB expression was significantly decreased in

DENA-Lf (200 mg/kg) and DENA-Lf (400 mg/kg)-treated groups (Fig. 5d and e, respectively) with mean IRS of  $2.60 \pm 0.22$  and  $1.40 \pm 0.42$ , respectively.

#### VEGF immunohistochemical staining

Positive staining for VEGF protein in the hepatic sinusoids and sparse hepatocytes of VHC group (Fig. 6a). While, DENA-treated group revealed weak expression for VEGF protein in the vicinity of tumor cells but relatively strong immune staining was demonstrated at the periphery of cancerous nodule (Fig. 6b) with mean IRS of  $3.40 \pm 0.42$ . Moderate expression of VEGF was recorded in DENA-Lf (100 mg/kg) (Fig. 6c) and DENA-Lf (200 mg/kg)-treated groups (Fig. 6d) with mean IRS of  $2.80 \pm 0.38$  and  $2.30 \pm 0.36$ , respectively, which is significantly different from DENA-treated one. On the other hand, significant weak expression of VEGF was recorded in DENA-Lf (400 mg/kg)-treated group (Fig. 6e) with mean IRS of  $1.80 \pm 0.24$ .

#### Caspase-3 immunohistochemical staining

Sparse immune immune reactive cells for caspase 3 was demonstrated in VHC-treated group (Fig. 7a). In contrast, moderate

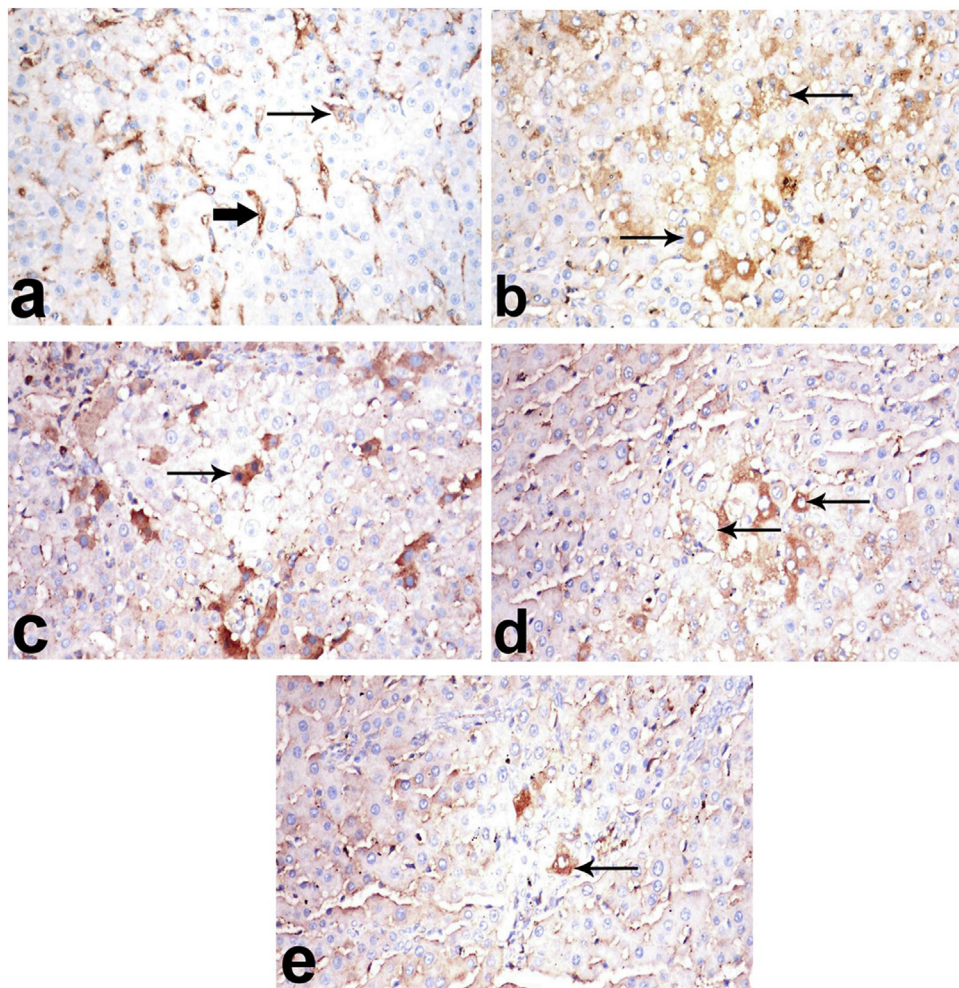


**Fig. 6.** VEGF immunohistochemical staining of liver tissues. VHC, rats treated with vehicles; DENA, rats treated with diethylnitrosamine; DENA-Lf, rats treated with diethylnitrosamine and lactoferrin; VEGF, vascular endothelial growth factor. (a) VHC-treated rats showing positive staining for VEGF protein in the hepatic sinusoids (thick arrow) and sparse hepatocytes (arrow), (b) DENA-treated rats showing relatively strong immune staining at the periphery of cancerous nodule (arrows), (c) DENA-Lf (100 mg/kg)-treated rats showing moderate expression of VEGF protein (arrows), (d) DENA-Lf (200 mg/kg)-treated rats showing moderate expression of VEGF protein (arrows), and (e) DENA-Lf (400 mg/kg)-treated rats showing weak expression of VEGF protein (arrows) (VEGF-immunohistochemical staining, X40).

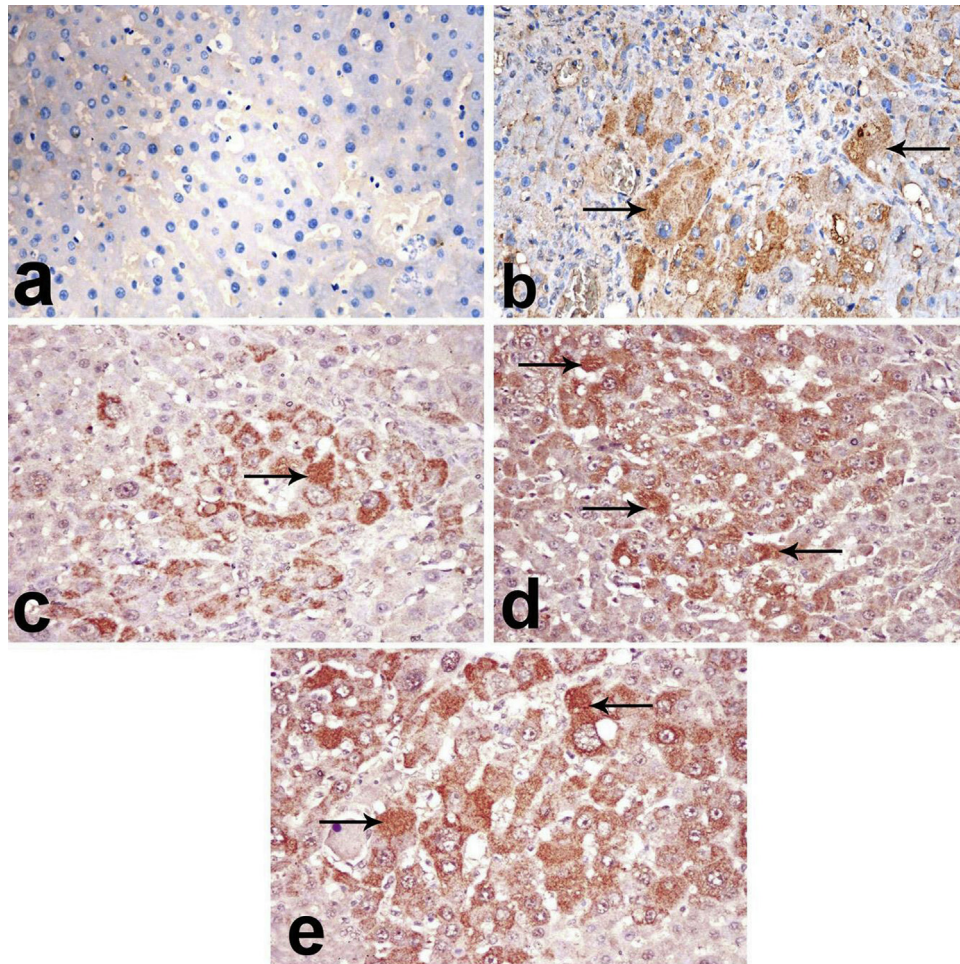


**Fig. 7.** Caspase-3 immunohistochemical staining of liver tissues. VHC, rats treated with vehicles; DENA, rats treated with diethylnitrosamine; DENA-Lf, rats treated with diethylnitrosamine and lactoferrin. (a) VHC-treated rats showing no immune reactive cells, (b) DENA-treated rats showing moderate expression of caspase-3 with cytoplasmic staining (arrows), (c) DENA-Lf (100 mg/kg)-treated rats showing moderate expression of caspase-3 with cytoplasmic and nuclear staining (arrows), (d) DENA-Lf (200 mg/kg)-treated rats showing remarkable increase of caspase-3 expression (arrows), and (e) DENA-Lf (400 mg/kg)-treated rats showing diffuse overexpression of caspase-3 (arrows) (Caspase-3 immunohistochemical staining, X40).

expression of caspase-3 was demonstrated in DENA and DENA-Lf (100 mg/kg)-treated groups (Fig. 7b and c, respectively), with nonsignificant difference between them, in which the mean IRS for both group was  $3.50 \pm 0.40$  and  $3.55 \pm 0.24$ , respectively. On the other hand, remarkable increase of caspase 3 expression was recorded in DENA-Lf (200 mg/kg)-treated group (Fig. 7d) and DENA-Lf (400 mg/kg) (Fig. 7e) with mean IRS of  $5.10 \pm 0.27$  and  $5.30 \pm 0.21$ , respectively, which is significantly different from DENA and DENA-Lf (100 mg/kg)-treated groups.

#### PCNA immunohistochemical staining

Scarse PCNA- positive cells were demonstrated in VHC-treated group ( $0.20 \pm 0.24$ ) (Fig. 8a), while significant increase of PCNA immune stained nuclei was recorded in DENA-treated group ( $89.40 \pm 5.09$ ) (Fig. 8b) compared to the VHC-treated group. On the contrary, decreased number of PCNA immune stained nuclei was recorded in DENA-Lf (100 mg/kg) treated group ( $49.20 \pm 5.81$ ) (Fig. 8c) which is significantly different from the DENA-treated one. Significant decrease of PCNA immune stained nuclei was recorded in DENA-Lf (200 mg/kg) and DENA-Lf (400 mg/kg) respectively ( $17.40 \pm 2.20$  and  $9.40 \pm 1.29$ , respectively) (Fig. 8d and 8e) which is significantly different from other treated groups.

#### *In vitro evaluation of the proliferation of DENA–HCC primary cell culture treated with PKB inhibitor, or PKB activator alone and in combination with Lf*

PKB inhibitor, Gsk690693 significantly reduced proliferation of DENA–HCC Cells compared to the negative control (CT-DENA–HCC) (Fig. 9a). A mild to moderate reduction were observed with 1 and 3 days of treatment, respectively. However, a more significant reduction was obtained on day 5.

Moreover, the effect of PKB activator (insulin) and its combination with Lf, on the growth rate of DENA–HCC cells is shown in Fig. 9b. Insulin treatment appeared to be effective and amplified the proliferation of DENA–HCC cells *in vitro* compared to the negative control. However, a statistically significant reduction in growth was observed in cells treated with a combination of the 2 drugs as early as 24 h after treatment.

#### Discussion

DENA is a well-known dietary carcinogen that is commonly used in induction of clinically relevant HCC in experimental animals [33]. Induction of HCC by DENA in the current study was evidenced by the biochemical, morphological, histopathological

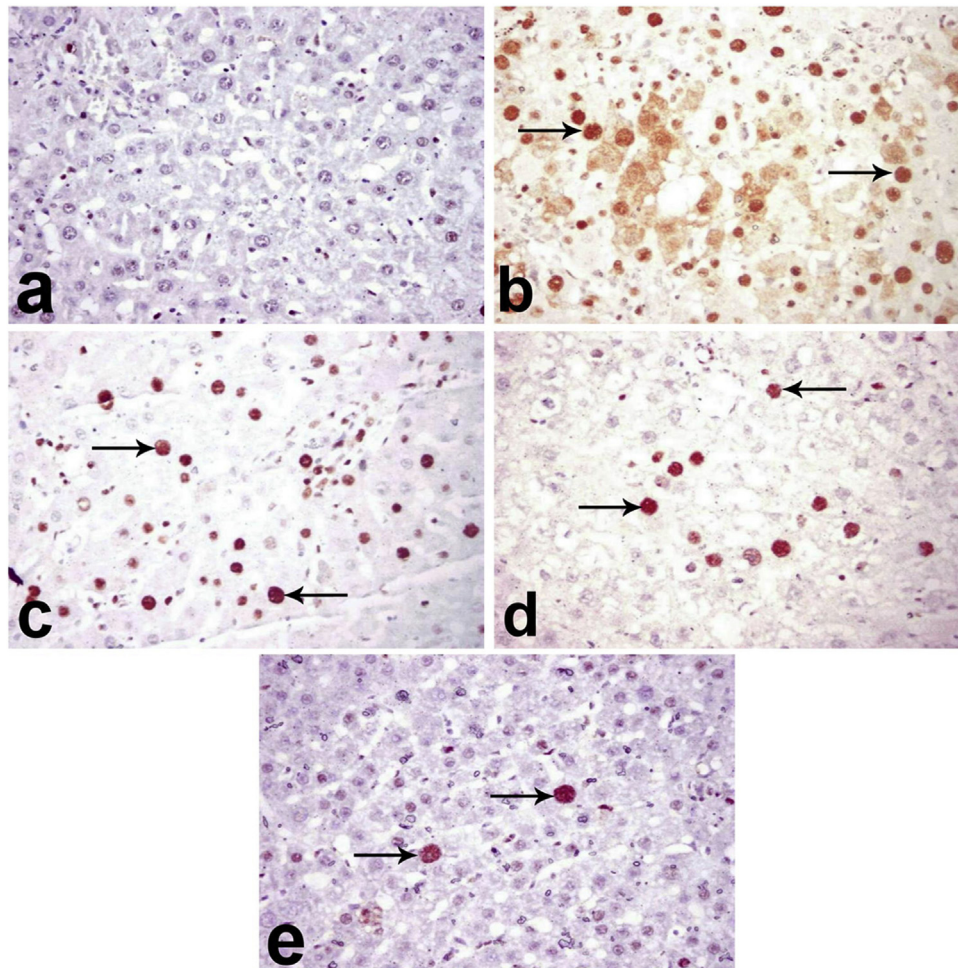


**Fig. 8.** PCNA immunohistochemical staining of liver tissues. VHC, rats treated with vehicles; DENA, rats treated with diethylnitrosamine; DENA-Lf, rats treated with diethylnitrosamine and lactoferrin; PCNA, proliferating cell nuclear antigen. (a) VHC-treated rats showing sparse immune reactive cells, (b) DENA-treated rats showing significant increase of PCNA immune stained nuclei (arrows), (c) DENA-Lf (100 mg/kg)-treated rats showing decreased number of PCNA immune stained nuclei (arrows), (d) DENA-Lf (200 mg/kg)-treated rats showing significant decrease of PCNA immune stained nuclei (arrows), and (e) DENA-Lf (400 mg/kg)-treated rats showing few scattered immune reactive cells (arrows) (PCNA immunohistochemical staining, X40).

and immunohistochemical findings. The elevation of the serum biomarkers of liver function indicated the hepatocellular damage and was in agreement with other studies [19,33]. ALT and AST are cytoplasmic in origin and physiologically detectable in serum with very low concentrations. Their abnormal serum amounts indicate cell membrane damage and hepatocytes death [34]. Also, hyperbilirubinemia indicates liver failure to conjugate and excrete bilirubin [35].

Moreover, increment of the hepatic oxidative index in the present DENA model indicated the exposure of the liver to oxidative stress, a factor that was reported as one of the major reasons contribute to the pathogenesis of HCC [36]. Furthermore, the increased levels of AFP and LDH in the liver indicated the induction of HCC. AFP is often measured as a tumor marker for diagnosis of HCC [37]. Also, LDH the enzyme that participates in the normal anaerobic glycolysis, is frequently increased in human cancers due to the overproduction of lactic acid by cancer cells; thus, it is considered as a tumor marker [38].

Morphometrically and histopathologically, a multi nodular pattern HCC was observed, and the immunohistochemical analysis revealed enhancement of proliferation with no augmentation of the normal apoptotic activity in the liver of DENA-treated group. The observed induction of HCC in this study using the DENA model is in line with the findings described in the other studies used the same model [6,39].

Inhibition of DENA-induced HCC by Lf was observed, as indicated by the improvement of the serum liver function biomarkers, as well as the hepatic nodulogenesis, oxidative index, and tumor markers levels. Histopathological and immunohistochemical investigations confirmed the biochemical outcome and revealed a dose-dependent inhibition of DENA-induced hepatocarcinogenesis and cell proliferation, and enhancement of apoptosis. However, though the presence of few malignant hepatic foci at the microscopic level in the livers of DEN-Lf treated rats, the reported normal levels of hepatic AFP suggesting them as premalignant foci, atypical non-AFP-positive hepatic lesions [40]. In line with the current findings, the antitumor activity of Lf is well reported, and its chemopreventive activity against HCC has been previously demonstrated [13,14]. Indubitably, the antioxidant property of Lf played an important role in the attenuation of the present hepatocarcinogenic effect of DENA, as revealed by the correction of the oxidative state of the liver. However, increasing evidence indicates the direct inhibition of tumor cell growth by Lf [10]; though, the molecular mechanism underlying this effect is incompletely understood.

Meanwhile, data support the suggestion that aberrant activation of PKB is involved in human cancers and that inhibition of PKB signaling pathway might be a promising strategy for cancer

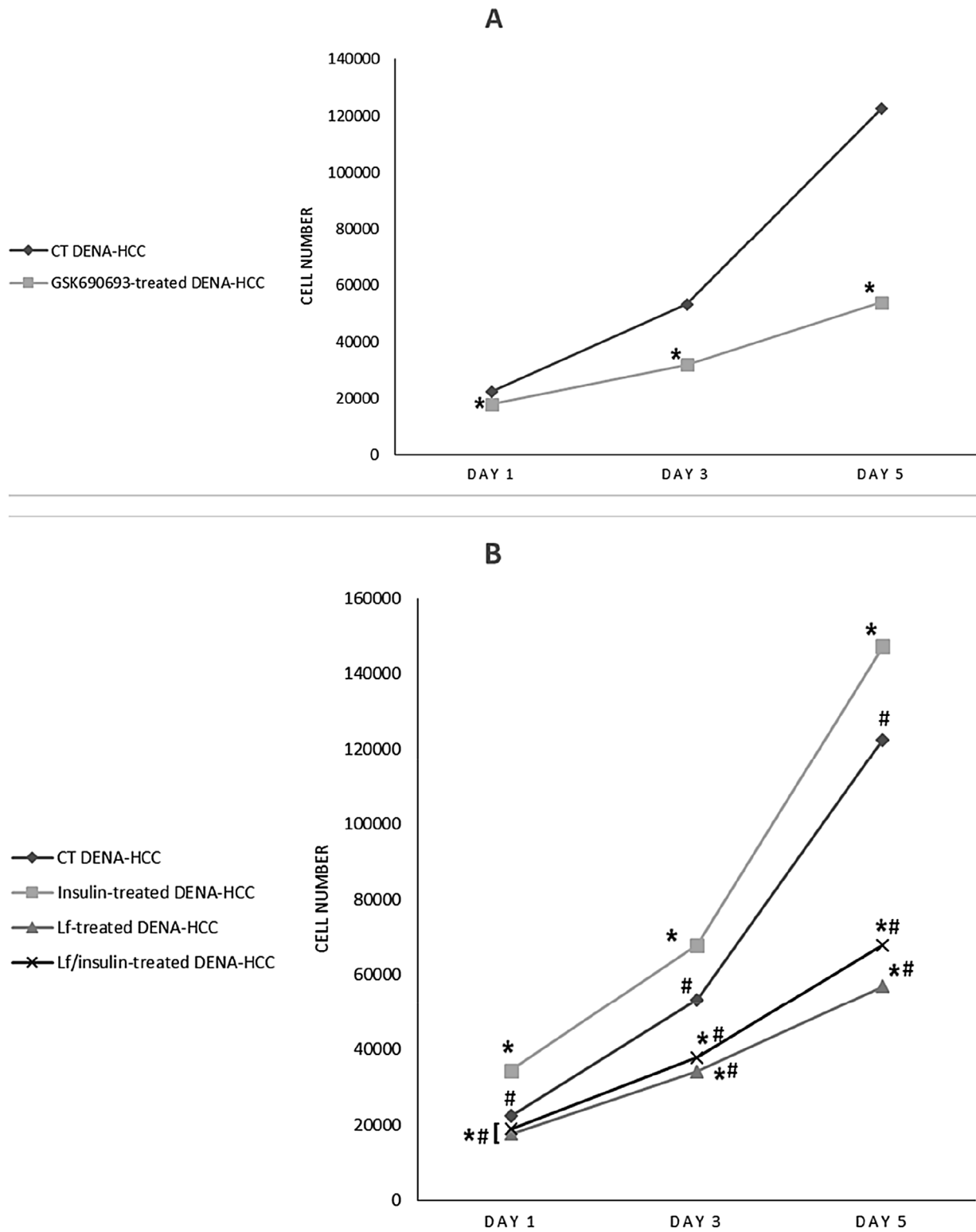


**Fig. 9.** Effect of drug treatments on the cell proliferation in DENA-HCC primary cell line (a) PKB inhibitor, (b) PKB activator alone and in combination with Lf. CT DENA-HCC, negative control DENA-HCC primary cell line treated with DMSO; GSK690693-treated DENA-HCC, DENA-HCC primary cell line treated with PKB inhibitor; Insulin-treated DENA-HCC, DENA-HCC primary cell line treated with PKB activator; Lf-treated DENA-HCC, DENA-HCC primary cell line treated with Lf; Lf/insulin-treated DENA-HCC, DENA-HCC primary cell line treated with Lf and PKB activator. Values represent the means  $\pm$  SE of 3 individual determinations. \*Significantly different from CT DENA-HCC at the corresponding day at  $p < 0.05$ . #Significantly different from Insulin-treated DENA-HCC at the corresponding day at  $p < 0.05$ .

treatment. PKB has been found to play an important role in carcinogenesis as it regulates cell-cycle progression, and prevents apoptosis through inhibition of caspase-3 [18,41]. Moreover, PKB has been found to direct the angiogenesis, the process of

generation of blood vessels that is essential for the survival and growth of the tumor cells in nutrient-depleted conditions. PKB activation contributes to this process through downstream activation of VEGF in endothelial cells in the lining of blood

vessels [42]. In addition, PKB activates eNOS, which increases production of nitric oxide that stimulates vasodilation and vascular remodeling [43].

Supporting these data explained the role of PKB in cancer formation, the findings of the present study showed that DENA model of HCC was associated with elevated hepatic levels of phosphorylated PKB. Investigation of its downstream activation products revealed raised levels of eNOS and enhanced expression of VEGF in the liver of HCC rats. These data point out the involvement of PKB pathway in increasing the cell proliferation and suppressing the apoptosis of the hepatocytes, and eventually in the hepatocarcinogenesis induced in rats by DENA. The findings of the current *in vitro* experiment confirmed the role of PKB in DENA-induced HCC, as the cell proliferation was reduced in the DENA–HCC primary cell culture treated with specific PKB inhibitor. As PKB is known to be activated due to the effect of oxidative stress, the activation of PKB in this HCC might be a result of DENA-induced reactive oxygen species-mediated PKB activation [44], a suggestion that is supported by the oxidative stress state observed in this study.

On the other hand, decreased levels of phosphorylated PKB, eNOS and VEGF were observed in Lf-treated groups, in a dose-dependent fashion, suggesting the inhibition of PKB activation and, subsequently, its signaling pathway by Lf. These effects were linked with the detected suppression of proliferation and induction of apoptosis via caspase-3 activation in HCC cells. Supportively, in the *in vitro* study, Lf showed inhibition of PKB activator-mediated cell proliferation in DENA–HCC primary cell culture, indicating a direct inhibition of PKB by Lf.

In line with our findings, decreased levels of phosphorylated PKB were also observed in association with Lf-induced growth inhibition of head and neck cancer cells [45]. Other study also demonstrated induction of apoptosis of stomach cancer cell and regulation of PKB signaling pathway by Lf, and suggested that Lf inhibits PKB activation and modulates its downstream proteins phosphorylation in cancer cells [46].

Stimulatingly, the direct effect of Lf on PKB observed in the present work can explain and link the findings of some older studies. In one of these studies, Damiens et al. demonstrated that Lf induces growth arrest of human breast carcinoma cells by inhibiting cyclin-dependent kinases that modulate the expression and the activity of key regulatory proteins in the cell-cycle progression [47]. Additionally, an increased expression of the cyclin-dependent kinases inhibitor proteins was reported in the same study. In other studies, it has been found that PKB increases the cell proliferation in breast cancer cells through inhibition of cyclin-dependent kinase inhibitor [48]. Taken together, our results could logically link the former findings and conclude that Lf-induced growth arrest and inhibition of cyclin-dependent kinases activity might be exerted through inhibition of PKB-mediated regulation of these kinases.

Interestingly, regulation of PKB activation by Lf does not only explain the direct anti-carcinogenic activity of Lf, however, it could also justify its previously reported anti-metastatic effect [49], as PKB is known to promote cancer metastasis [50]

## Conclusion

This study revealed a significant dose-dependent chemopreventive effect of Lf against DENA-initiated and PhB-promoted HCC in rats. The well-recounted antioxidant activity of Lf was confirmed by the results of the current experiment, and it is suggested to play a role in this anti-tumor activity of Lf. Interestingly, our finding demonstrated that, *in vivo*, Lf decreased the level and expression of phosphorylated PKB in the hepatocytes in the rat model of DENA-induced HCC. In addition, Lf reduced the

expression and activation of eNOS, VEGF, which are activated through PKB downstream signaling pathway, and enhanced the activation of caspase-3 that is blocked by PKB. Also, *in vitro*, Lf has been found to reduce the PKB-mediated cell progression in DENA–HCC primary cell culture. Taken together, these findings suggest that Lf directly regulates the activation of PKB and subsequently inhibits its mediated actions, and propose this activity of Lf as a potential mechanism involved in its direct anti-carcinogenic capacity.

## Author contributions

RH: Conceptualization; Data curation; Formal analysis; Funding acquisition; Investigation; Methodology; Project administration; Resources; Roles/Writing–original draft; Writing–review and editing. DF: Investigation; Methodology; Formal analysis; Resources; Writing – review and editing. AS: Investigation; Methodology; Resources; Formal analysis. RA: Investigation; Methodology; Resources; Formal analysis. AH: Histopathological analysis; Resources.

## Conflict of interest

The authors declare no potential conflicts of interest.

## Acknowledgment

This study was supported by the National Research Centre (Giza, Egypt), grant number P100517.

## References

- [1] Parkin DM. Global cancer statistics in the year 2000. *Lancet Oncol* 2001;2:533–43.
- [2] Okuda K, Nakanuma Y, Miyazaki M. Cholangiocarcinoma: recent progress. Part 1: epidemiology and etiology. *J Gastroenterol Hepatol* 2002;17:1049–55.
- [3] Perz JF, Armstrong GL, Farrington LA, Hutin YJ, Bell BP. The contributions of hepatitis B virus and hepatitis C virus infections to cirrhosis and primary liver cancer worldwide. *J Hepatol* 2006;45:529–38.
- [4] Alazawi W, Cunningham M, Dearden J, Foster GR. Systematic review: outcome of compensated cirrhosis due to chronic hepatitis C infection. *Aliment Pharmacol Ther* 2010;32:344–55.
- [5] Farazi PA, DePinho RA. Hepatocellular carcinoma pathogenesis: from genes to environment. *Nat Rev Cancer* 2006;6:674–87.
- [6] Kensler TW, Egner PA, Wang JB, Zhu YR, Zhang BC, Lu PX, et al. Chemoprevention of hepatocellular carcinoma in aflatoxin endemic areas. *Gastroenterology* 2004;127:S310–8.
- [7] Yates MS, Kensler TW. Keap1 eye on the target: chemoprevention of liver cancer. *Acta Pharmacol Sin* 2007;28:1331–42.
- [8] Levay PF, Viljoen M. Lactoferrin: a general review. *Haematologica* 1995;80:252–67.
- [9] Gonzalez-Chavez SA, Arevalo-Gallegos S, Rascon-Cruz Q. Lactoferrin: structure, function and applications. *Int J Antimicrob Agents* 2009;33(301):e1–8.
- [10] Fang B, Zhang M, Tian M, Jiang L, Guo HY, Ren FZ. Bovine lactoferrin binds oleic acid to form an anti-tumor complex similar to HAMLET. *Biochim Biophys Acta* 2014;1841:535–43.
- [11] Shi H, Li W. Inhibitory effects of human lactoferrin on U14 cervical carcinoma through upregulation of the immune response. *Oncol Lett* 2014;7:820–6.
- [12] Gifford JL, Hunter HN, Vogel HJ. Lactoferrin: a lactoferrin-derived peptide with antimicrobial, antiviral, antitumor and immunological properties. *Cell Mol Life Sci* 2005;62:2588–98.
- [13] Gibbons JA, Kanwar RK, Kanwar JR. Lactoferrin and cancer in different cancer models. *Front Biosci (Schol Ed)*. 2011;3:1080–8.
- [14] Fujita K, Ohnishi T, Sekine K, Iigo M, Tsuda H. Down-regulation of 2-amino-3,8-dimethylimidazo[4,5-f]quinoxaline (MeIQx)-induced CYP1A2 expression is associated with bovine lactoferrin inhibition of MeIQx-induced liver and colon carcinogenesis in rats. *Jpn J Cancer Res* 2002;93:616–25.
- [15] El-Fakharany EM, Sanchez L, Al-Mehdar HA, Redwan EM. Effectiveness of human, camel, bovine and sheep lactoferrin on the hepatitis C virus cellular infectivity: comparison study. *Virology* 2013;10:199.
- [16] Wei M, Guo X, Tu L, Zou Q, Li Q, Tang C, et al. Lactoferrin-modified PEGylated liposomes loaded with doxorubicin for targeting delivery to hepatocellular carcinoma. *Int J Nanomedicine* 2015;10:5123–37.
- [17] Testa JR, Tschlis PN. AKT signaling in normal and malignant cells. *Oncogene* 2005;24:7391–3.
- [18] Prasad S, Madan E, Nigam N, Roy P, George J, Shukla Y. Induction of apoptosis by lupeol in human epidermoid carcinoma A431 cells through regulation of

- mitochondrial, Akt/PKB and NFκB signaling pathways. *Cancer Biol Ther* 2009;8:1632–9.
- [19] Hussein UK, Mahmoud HM, Farrag AG, Bishayee A. Chemoprevention of diethylnitrosamine-initiated and phenobarbital-promoted hepatocarcinogenesis in rats by sulfated polysaccharides and aqueous extract of *Ulva lactuca*. *Integr Cancer Ther* 2015;14:525–45.
- [20] Hessin A, Hegazy R, Hassan A, Yassin N, Kenawy S. Lactoferrin enhanced apoptosis and protected against thioacetamide-induced liver fibrosis in rats. *Open Access Maced J Med Sci* 2015;3:195–201.
- [21] Hegazy R, Salama A, Mansour D, Hassan A. Renoprotective effect of lactoferrin against chromium-induced acute kidney injury in rats: involvement of IL-18 and IGF-1 inhibition. *PLoS One* 2016;11:e0151486.
- [22] Wellington D, Mikaelian I, Singer L. Comparison of ketamine-xylazine and ketamine-dexmedetomidine anesthesia and intraperitoneal tolerance in rats. *J Am Assoc Lab Anim Sci* 2013;52:481–7.
- [23] Bishayee A, Chatterjee M. Inhibition of altered liver cell foci and persistent nodule growth by vanadium during diethylnitrosamine-induced hepatocarcinogenesis in rats. *Anticancer Res* 1995;15:455–61.
- [24] Stewart HL, Snell KC. The histopathology of experimental tumors of the liver of the rat; a critical review of the histopathogenesis. *Acta Unio Int Contra Cancrum* 1957;13:770–803.
- [25] Bhattacharya S, Chatterjee M. Protective role of *Trianthema portulacastrum* against diethylnitrosamine-induced experimental hepatocarcinogenesis. *Cancer Lett* 1998;129:7–13.
- [26] Maae E, Nielsen M, Steffensen KD, Jakobsen EH, Jakobsen A, Sorensen FB. Estimation of immunohistochemical expression of VEGF in ductal carcinomas of the breast. *J Histochem Cytochem* 2011;59:750–60.
- [27] Li W, Fan Q, Ma B, Ren M, Li H, Gou Y, et al. [An animal model of Perthes disease and an experimental research of VEGF expression]. *Zhongguo Xiu Fu Chong Jian Wai Ke Za Zhi* 2008;22:814–9.
- [28] Cheung PF, Yip CW, Ng LW, Lo KW, Wong N, Choy KW, et al. Establishment and characterization of a novel primary hepatocellular carcinoma cell line with metastatic ability in vivo. *Cancer Cell Int* 2014;14:103.
- [29] Li K, Qu X, Wang Y, Tang Y, Qin D, Wang Y, et al. Improved performance of primary rat hepatocytes on blended natural polymers. *J Biomed Mater Res A* 2005;75:268–74.
- [30] Levy DS, Kahana JA, Kumar R. AKT inhibitor, GSK690693, induces growth inhibition and apoptosis in acute lymphoblastic leukemia cell lines. *Blood* 2009;113:1723–9.
- [31] Arcella A, Oliva MA, Staffieri S, Aalberti S, Grillea G, Madonna M, et al. In vitro and in vivo effect of human lactoferrin on glioblastoma growth. *J Neurosurg* 2015;123:1026–35.
- [32] He Y, Tan X, Hu H, Wang Q, Hu X, Cai X, et al. Metformin inhibits the migration and invasion of esophageal squamous cell carcinoma cells by downregulating the protein kinase B signaling pathway. *Oncol Lett* 2018;15:2939–45.
- [33] Sayed-Ahmed MM, Aleisa AM, Al-Rejaie SS, Al-Yahya AA, Al-Shabanah OA, Hafez MM, et al. Thymoquinone attenuates diethylnitrosamine induction of hepatic carcinogenesis through antioxidant signaling. *Oxid Med Cell Longev* 2010;3:254–61.
- [34] Hoekstra LT, de Graaf W, Nibourg GA, Heger M, Bennink RJ, Stieger B, et al. Physiological and biochemical basis of clinical liver function tests: a review. *Ann Surg* 2013;257:27–36.
- [35] Alshawsh MA, Abdulla MA, Ismail S, Amin ZA. Hepatoprotective effects of Orthosiphon stamineus extract on thioacetamide-induced liver cirrhosis in rats. *Evid Based Complement Alternat Med* 2011;2011:103039.
- [36] Kawanishi S, Hiraku Y, Pinlaor S, Ma N. Oxidative and nitrative DNA damage in animals and patients with inflammatory diseases in relation to inflammation-related carcinogenesis. *Biol Chem* 2006;387:365–72.
- [37] Johnson PJ. The role of serum alpha-fetoprotein estimation in the diagnosis and management of hepatocellular carcinoma. *Clin Liver Dis (Hoboken)* 2001;5:145–59.
- [38] Miao P, Sheng S, Sun X, Liu J, Huang G. Lactate dehydrogenase A in cancer: a promising target for diagnosis and therapy. *IUBMB Life* 2013;65:904–10.
- [39] Bishayee A, Barnes KF, Bhatia D, Darvesh AS, Carroll RT. Resveratrol suppresses oxidative stress and inflammatory response in diethylnitrosamine-initiated rat hepatocarcinogenesis. *Cancer Prev Res (Phila)* 2010;3:753–63.
- [40] Sell S. Distribution of alpha-fetoprotein- and albumin-containing cells in the livers of Fischer rats fed four cycles of N-2-fluorenylacetamide. *Cancer Res* 1978;38:3107–13.
- [41] Zhang HM, Rao JN, Guo X, Liu L, Zou T, Turner DJ, et al. Akt kinase activation blocks apoptosis in intestinal epithelial cells by inhibiting caspase-3 after polyamine depletion. *J Biol Chem* 2004;279:22539–47.
- [42] Tsutsui S, Matsuyama A, Yamamoto M, Takeuchi H, Oshiro Y, Ishida T, et al. The Akt expression correlates with the VEGF-A and -C expression as well as the microvessel and lymphatic vessel density in breast cancer. *Oncol Rep* 2010;23:621–30.
- [43] Tanimoto T, Jin ZG, Berk BC. Transactivation of vascular endothelial growth factor (VEGF) receptor Flk-1/KDR is involved in sphingosine 1-phosphate-stimulated phosphorylation of Akt and endothelial nitric-oxide synthase (eNOS). *J Biol Chem* 2002;277:42997–3001.
- [44] Hou J, Cui A, Song P, Hua H, Luo T, Jiang Y. Reactive oxygen species-mediated activation of the Src-epidermal growth factor receptor-Akt signaling cascade prevents bortezomib-induced apoptosis in hepatocellular carcinoma cells. *Mol Med Rep* 2015;11:712–8.
- [45] Xiao Y, Monitto CL, Minhas KM, Sidransky D. Lactoferrin down-regulates G1 cyclin-dependent kinases during growth arrest of head and neck cancer cells. *Clin Cancer Res* 2004;10:8683–6.
- [46] Xu XX, Jiang HR, Li HB, Zhang TN, Zhou Q, Liu N. Apoptosis of stomach cancer cell SGC-7901 and regulation of Akt signaling way induced by bovine lactoferrin. *J Dairy Sci* 2010;93:2344–50.
- [47] Damiens E, El Yazidi I, Mazurier J, Duthille I, Spik G, Boilly-Marer Y. Lactoferrin inhibits G1 cyclin-dependent kinases during growth arrest of human breast carcinoma cells. *J Cell Biochem* 1999;74:486–98.
- [48] Viglietto G, Motti ML, Bruni P, Melillo RM, D'Alessio A, Califano D, et al. Cytoplasmic relocation and inhibition of the cyclin-dependent kinase inhibitor p27(Kip1) by PKB/Akt-mediated phosphorylation in breast cancer. *Nat Med* 2002;8:1136–44.
- [49] Iigo M, Kuhara T, Ushida Y, Sekine K, Moore MA, Tsuda H. Inhibitory effects of bovine lactoferrin on colon carcinoma 26 lung metastasis in mice. *Clin Exp Metastasis* 1999;17:35–40.
- [50] Kim D, Kim S, Koh H, Yoon SO, Chung AS, Cho KS, et al. Akt/PKB promotes cancer cell invasion via increased motility and metalloproteinase production. *FASEB J* 2001;15:1953–62.